Journal of Solid State Chemistry **151,** 31–39 (2000)
doi:10.1006/jssc.1999.8618, available online at http://www.idealibrary.com on IDEAL®

Synthesis, Structure, and Magnetic Behavior of $La_5Re_3MnO_{16}$: A New Perovskite-like Material

C. R. Wiebe, A. Gourrier, T. Langet, J. F. Britten, and J. E. Greedan[1]

The Brockhouse Institute for Materials Research, McMaster University, Hamilton, Ontario L8S 4M1, Canada

Received August 25, 1999; in revised form December 1, 1999; accepted December 15, 1999

Single crystals of $La_5Re_3MnO_{16}$ have been grown and characterized by X-ray diffraction. The crystal structure was found to be of triclinic symmetry, but with strong monoclinic pseudosymmetry and related to the structure of $La_5Mo_4O_{16}$ (M. Ledesert, Ph. Labbe, W. H. McCarroll, H. Leligny, and B. Raveau, *J. Solid State Chem.* 105, 143 (1993)). The atomic parameters were refined in the unconventional *C*-1 space group, which is derived from *C*2/*m* by suppressing the two-fold axis. The structure is similar to that of the perovskites, consisting of layers of slightly distorted corner-sharing ReO_6 and MnO_6 octahedra. The layers are connected by Re_2O_{10} units which consist of distorted edge-sharing ReO_6 octahedra. The Re–Re bond in these units is found to be unusually short (2.4068(5) Å). The La atoms are in three different crystallographic environments. La(1) and La(2) are eight- and seven-fold coordinated, respectively, and lie in chains in the ReO_6 and MnO_6 network. La(3) has a distorted cubic coordination in a cage formed by the Re_2O_{10} units. Bond valence sums are consistent with Mn^{2+} and Re^{5+}. Powder samples have also been synthesized for magnetic susceptibility measurements. The magnetic properties are complex. Curie–Weiss behavior occurs only in the range 400–600 K giving $C = 4.43$ emu · K/mol and $\theta = -48(5)$ K, consistent with Mn^{2+} as the only magnetic ion and net antiferromagnetic coupling. A transition to a long-range ordered state occurs below 160 K and a field-induced irreversibility sets in below 50 K. Isothermal magnetization-field data imply a complex H–T phase diagram and magnetic structure.

***Key Words*: perovskite-related structures; magnetism in lanthanum rhenium oxides.**

INTRODUCTION

The great interest in perovskite and layered pervoskite-like materials over the last several decades in solid state chemistry has been driven by frequent discoveries of the fascinating electronic and magnetic properties that they possess (1, 2). The accommodating nature of the octahedral framework of this structure has led to a plethora of compounds with a wide variety of physical properties by varying the cations A and B in the ABX_3 formula. Mixed valence materials have in particular shown promise as new candidates for exotic superconducting and magnetic ground states. The synthesis of lanthanum-transition metal oxides of mixed valence, for example, has led to the discovery of the celebrated high T_c superconducting ceramic $La_{2-x}Ba_xCuO_4$ (3) and other materials with low-dimensional electronic properties, such as $La_4Re_6O_{19}$ (4), which both have pervoskite-related structures. Although there are many such examples in the literature, new compounds are continually being discovered in this vast field of solid state science. This paper reports the synthesis of a new pervoskite-like material, $La_5Re_3MnO_{16}$, which consists of two distinct layers: a rhenium–manganese layer of corner-shared octahedra and a rhenium–rhenium layer of edge-shared bioctahedra. The magnetic properties have also been investigated and the results point to a complex behavior.

EXPERIMENTAL

Preparation of $La_5Re_3MnO_{16}$

Single crystals of $La_5Re_3MnO_{16}$ resulted during attempts to prepare La_3ReO_7 from a reactant mixture composed of stoichiometric ratios of La_2O_3, ReO_3, and ReO_2. A pellet of MnO_2, intended to function as an oxygen source, was wrapped in platinum foil and included in the reaction tube. The powder mixture was well homogenized and pressed into a pellet, which was then placed in a sealed platinum tube under an argon atmosphere. The reaction was carried out at 1400°C for 12 h. The product was a black powder containing small plate-like crystals, which were investigated under polarized light for quality. The chemical composition was confirmed to be $La_5Re_3MnO_{16}$ by X-ray diffraction, which indicated unintentional mixing of the two pellets.

The synthesis of polycrystalline $La_5Re_3MnO_{16}$ was accomplished by the following reaction:

$$5La_2O_3 + 3ReO_2 + 3ReO_3 + 2MnO \rightarrow 2La_5Re_3MnO_{16}. \quad [1]$$

[1] To whom correspondence should be addressed.

0022-4596/00 $35.00

The reactants were mixed well and pressed into pellets, which were then sealed in a quartz tube under vacuum (5×10^{-5} Torr). The final product was obtained by two firings at 1050°C for 48 h, with an intermediate regrinding stage. The resulting sample was found to clearly contain two phases—an outer transparent layer of material and a small amount of black powder within. The black powder was found to be the compound of interest.

Magnetic Measurements

Magnetic measurements were performed on the polycrystalline sample using a Quantum Design MPMS SQUID magnetometer. Field cooled (FC) and zero field cooled runs (ZFC) were done in a temperature range 2 to 600 K in an applied magnetic field of 0.05 T. Magnetization runs as a function of field were also done up to fields of 5.5 T.

X.-Ray Powder Diffraction

The polycrystalline product was examined using a Guinier–Hagg camera with Cu$K\alpha_1$ radiation (λ = 1.54056 Å) and silicon as an internal standard. The lattice constants were refined using the program LSUDF, and reasonable agreement was found with the single crystal measurements ($a = 7.984(7)$ Å, $b = 8.020(3)$ Å, $c = 10.255(8)$ Å, $\alpha = 90.19(4)°$, $\beta = 95.29(3)°$, $\gamma = 90.17(4)°$).

Single crystal X-ray diffraction data were collected using a P4 Siemens diffractometer on a Mo$K\alpha$ rotating anode source ($\lambda = 0.71073$ Å) which was equipped with a 1 K charge-coupled device (CCD) area detector. The software programs SAINT and SADABS were used to account for the three-dimensional Lorentz and polarization factors and the absorption corrections, respectively. Face-indexed absorption corrections were applied at a later stage in view of the plate-like habit of the crystals. The crystal structure was solved using the SHELXTL 5.03 software package.

RESULTS AND DISCUSSION

Crystal Structure

The unit cell of $La_5Re_3MnO_{16}$ was found to possess triclinic symmetry with unit cell parameters $a = 7.9885(5)$ Å, $b = 8.0322(5)$ Å, $c = 10.2413(5)$ Å, $\alpha = 90.200(1)°$, $\beta = 95.160(2)°$, and $\gamma = 89.920(2)°$. The above parameters are very similar to those reported for $La_5Mo_4O_{16}$ which was described in the monoclinic space group $C2/m$, so an initial model was based on the structure of this compound (5). The refinement was ultimately improved by lowering the symmetry to the unconventional C-1 space group. The results from the final refinement are listed in Table 1, with a final R factor of 0.0343 and an R_w factor of 0.0854. The atomic positions were determined in this space group and are listed in Table 2.

TABLE 1

Crystal size and shape	$124 \times 94 \times 3$ μm, thin black plate
Lattice parameters	$a = 7.9885(5)$ Å, $b = 8.0322(5)$ Å, $c = 10.2413(5)$ Å, $\alpha = 90.200(1)°$, $\beta = 95.160(2)°$, $\gamma = 89.920(2)°$, $V = 654.47(7)$ Å^3
Space group	C-1
D_c; Z	7.937 g/cm; 2
Data collection technique	Siemens P4 diffractometer
Scan mode	θ–ϕ
Wavelength	Mo($K\alpha$) $\lambda = 0.71073$ Å
Number of measured reflections	7590, $-13 < h < 11$, $-13 < k < 10$, $-16 < l < 15$
Number of reflections used in refinement	3021 with $I > 2\sigma(I)$
Absorption corrections	Face-indexed correction based on crystal morphology
Absorption coefficient	μ (Mo$K\alpha$) $\sim 44.567\ cm^{-1}$
R, R_w	0.0343, 0.0854
$(\text{Shift/e.s.d})_{max}$	<0.001

Figure 1 shows a projection of the crystal structure of $La_5Re_3MnO_{16}$ along the [0 0 1] direction. The structure is related to the pervoskites, with a layered stacking of two distinct motifs in the a–b plane. One layer consists of octahedrally coordinated rhenium and manganese atoms, which are interconnected by corner-sharing oxygen atoms. Each rhenium unit is connected to four manganese units in the a–b plane, with two apexes that are free. The manganese units are likewise linked to the rhenium units in the a–b basal plane and are also linked to rhenium layers that lie above and below the rhenium–manganese layer. Figure 2 shows this explicitly as a projection of the structure along the [0 1 0] direction.

The octahedra in the rhenium–manganese layer exhibit a slight misalignment of their equatorial planes with the a–b plane of the unit cell (the distortion is quite distinct when viewed from the [0 1 0] direction). This misalignment is

TABLE 2

Atom	x	y	z	B (Å)^2
La(1)	0.22985(4)	0.74460(4)	0.80072(4)	0.00999(8)
La(2)	0.23097(4)	0.26311(4)	0.79498(4)	0.00858(8)
La(3)	0.5	0.5	0.5	0.00835(10)
Re(1)	0.05587(3)	0.50019(2)	0.39472(2)	0.00475(7)
Re(2)	0	0	0	0.00679(8)
Mn	0	0.5	0	0.0065(2)
O(1)	0.1910(5)	0.5020(6)	0.5651(4)	0.0083(7)
O(2)	0.2754(5)	0.5022(5)	0.3262(4)	0.0075(7)
O(3)	−0.0432(6)	0.4996(5)	0.2023(4)	0.0083(7)
O(4)	0.0716(6)	0.0012(6)	0.1827(5)	0.0101(8)
O(5)	0.0340(6)	0.7342(5)	0.3676(4)	0.0083(7)
O(6)	0.0403(6)	0.2645(5)	0.3670(5)	0.0089(7)
O(7)	−0.0565(6)	0.2420(5)	0.0039(5)	0.0123(9)
O(8)	0.2322(5)	0.0548(6)	−0.0348(5)	0.0114(8)

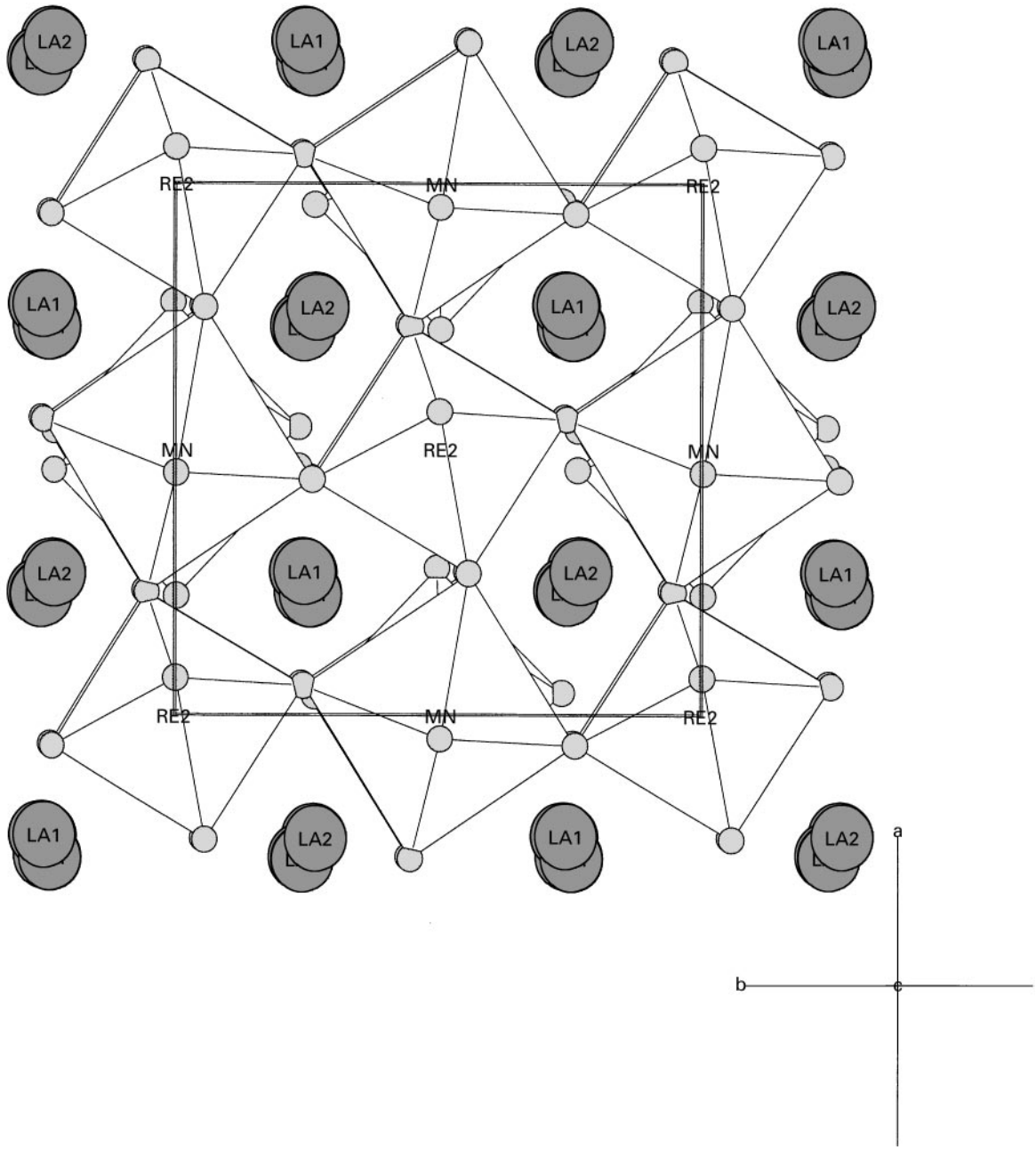

FIG. 1. Projection along [0 0 1].

significant since it plays a vital role in the determination of the proper space group of this crystal. Other refinements of the crystal structure were attempted in the monoclinic space groups *Cm* and *C*2/*m*. All of these refinements seemed to be reasonable, but upon closer examination it was deduced that this distortion of the octahedra breaks the mirror symmetry at [0 1 0]. Consequentially, the residuals of these monoclinic refinements would split the oxygen positions (O(8)) and therefore suggest that there is disorder at these sites (see Fig. 3). This was the approach of Ledesert *et al.* (5) who solved the structure of $La_5Mo_4O_{16}$ in *C*2/*m* with disorder at the same oxygen site. The conclusion that is reached here is that the distortion appears to be real in this material and is significant enough to lower the symmetry to a triclinic, *C*-1 space group (the twisting of the octahedra that is observed is typical in pervoskite structures with relatively small cations such as La). Attempts were made to refine the structure in monoclinic symmetry with disorder on O(8), but these were ultimately abandoned due to indications that the crystal was indeed triclinic (with strong

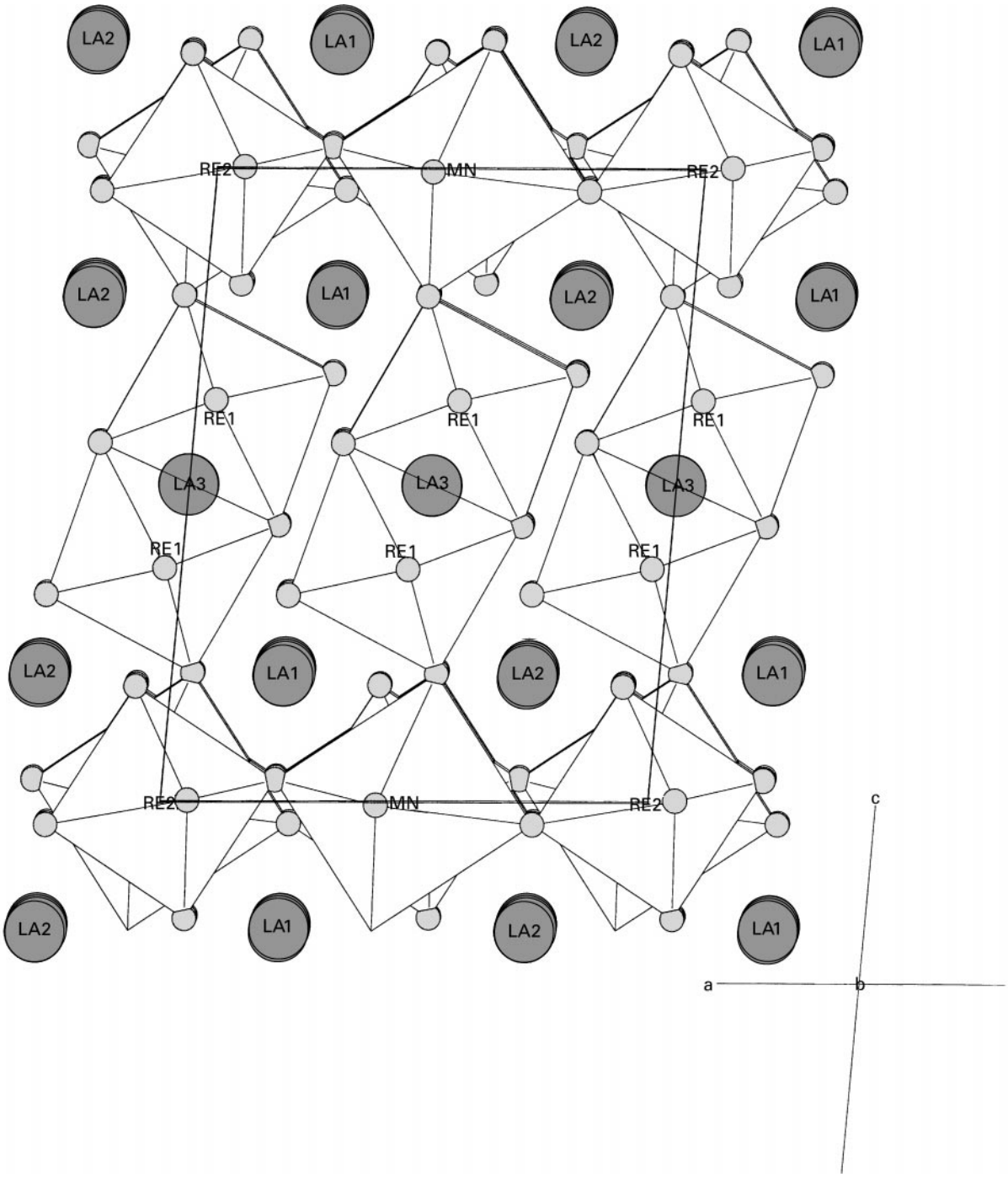

FIG. 2. Projection along [0 1 0].

angular deviations from 90° for α and γ), and the distortions of the octahedra in this layer appear to be genuine.

One of the more interesting aspects of this crystal structure lies in the consecutive layer of rhenium atoms, which are connected in dimers of edge-sharing octahedra. The close proximity of the octahedra causes a notable distortion of the oxygen positions, as noted in Fig. 4. It also leads to an off-centering of the rhenium atoms and thus an exceptionally short Re–Re bond distance of 2.4068(5) Å. Such short bond distances in edge-shared octahedra have been observed for Ti–Ti bonds in $Nd_3Ti_4O_{12}$ (2.760(3) Å) (6) and for Mo–Mo bonds in the $La_5Mo_4O_{16}$ structure, which were reported to be 2.406 Å by Ledesert *et al.* (5). There are also reports of extremely short Re–Re bonds in other La–Re–O

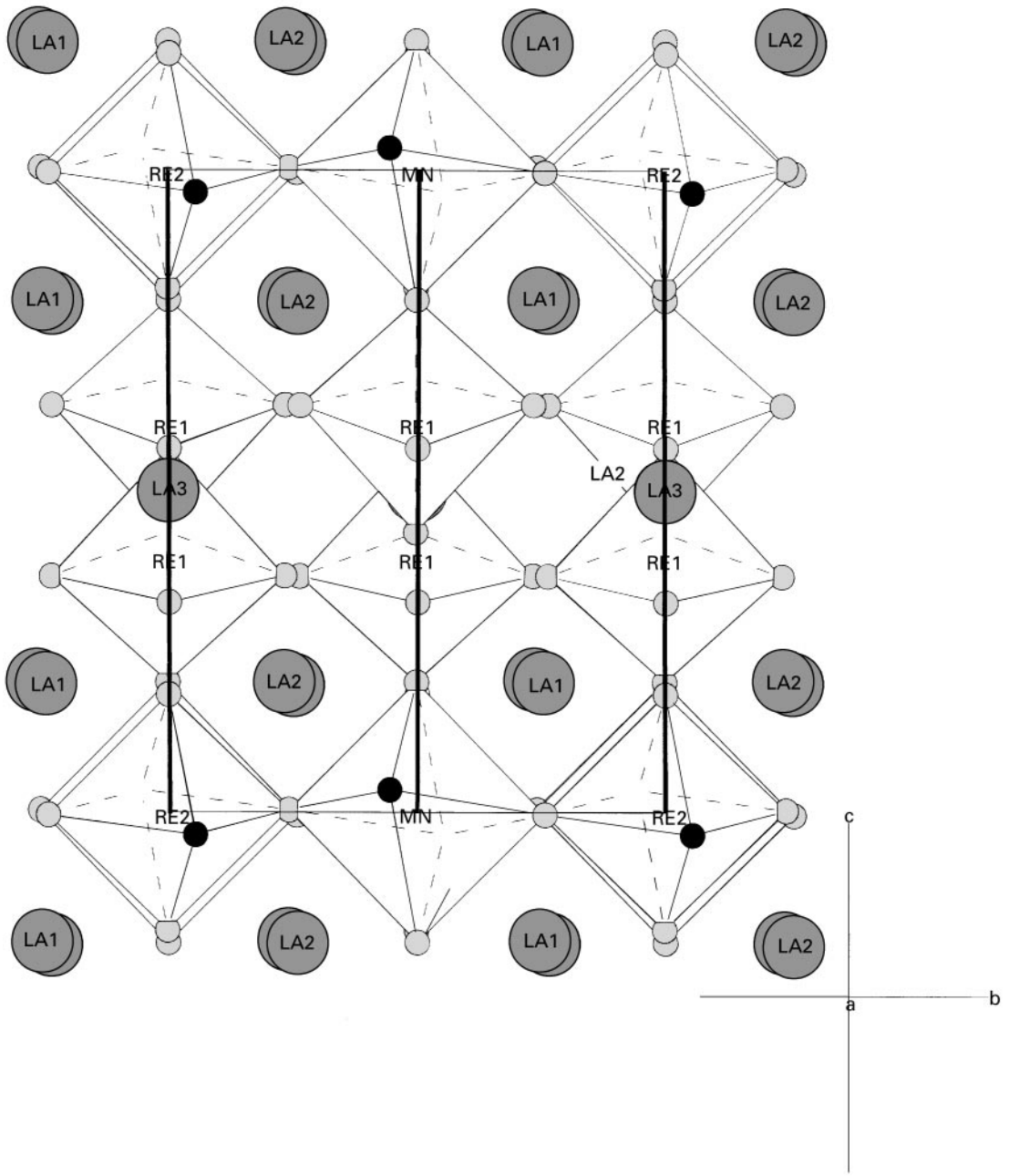

FIG. 3. Projection along [1 0 0] indicating where the mirror planes occur for the space group $C2/m$ (bold lines). Note the positions of O(8), oxygen positions in bold, that do not obey the mirror plane symmetries at $b = 0$, $b = 0.5$, and $b = 1.0$ and thus lower the symmetry of the crystal structure to C-1.

systems such as $La_6Re_4O_{18}$, $La_4Re_6O_{19}$, and $La_3Re_2O_{10}$ (7). In the case of $La_4Re_6O_{19}$, isolated edge-sharing units of rhenium–oxygen octahedra of the crystallographic formula Re_2O_{10} are observed in the same manner as our material. The Re–Re bond distance reported, 2.42 Å, is in good agreement with the bond distance in $La_5Re_3MnO_{16}$, and it is interpreted as a true metal–metal bond. Strong distortions of the oxygen positions are observed as well, with the Re atoms similarly displaced from the centers of their respective octahedra. The nature of the bonding can not be ascertained with the data presented here, but double or triple Re–Re bonding may indeed be present. Quadruple Re–Re bonds have been observed in other exotic materials such as the rhenium halides (i.e., $K_2Re_2Cl_8$) (7), but these are usually characterized by very short Re–Re bond distances on the order of 2.2 Å or less and are very rare.

The lanthanum atoms are found to reside in three distinct crystallographic sites. The La(1) and La(2) atoms are

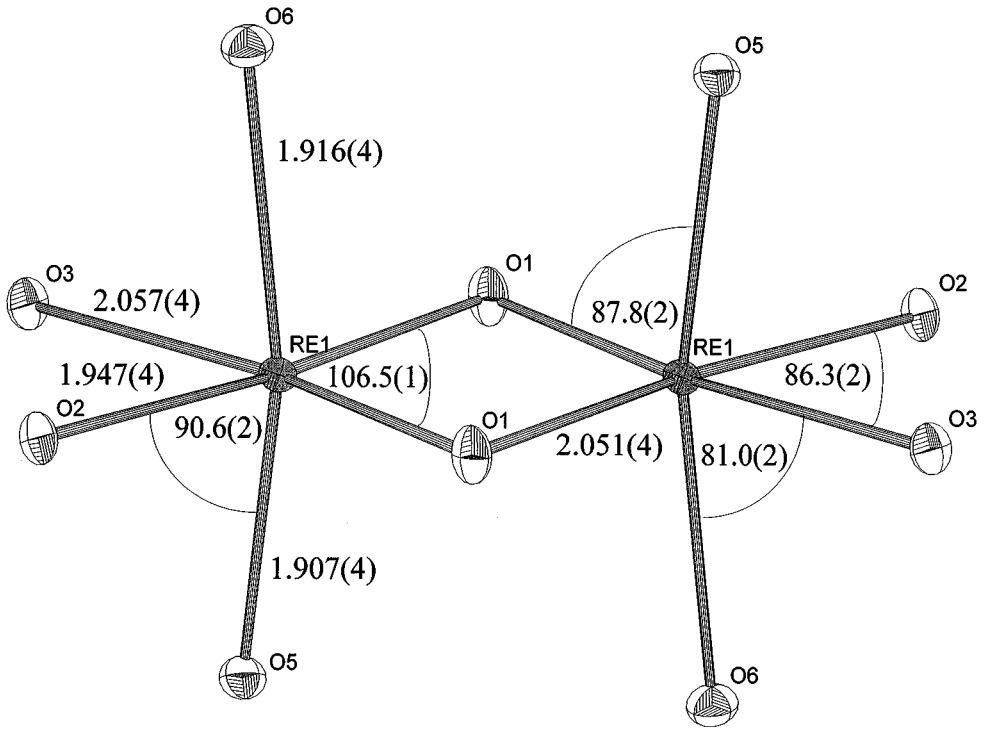

FIG. 4. The Re–Re bioctahedra. The edge-sharing of the octahedra provides significant distortions as indicated by the deviations of the angles from their ideal values. It is believed that the close proximity of the Re atoms (2.4068(5) Å) is evidence for a true Re–Re bond.

distributed in chains along the [0 1 0] direction that lie in the interstitial positions in the $Re(2)O_6$ and MnO_6 framework. For ease of presentation, the polyhedra that correspond to the coordination of the lanthanum atoms have been omitted from the figures, but they are seven- and eightfold coordinated, respectively, with oxygen. The La(3) atoms are located in cages delimited by the $Re(1)_2O_{10}$ dimers and thus possess a distorted cubic coordination.

All of the relevant bonds and bond angles for the atomic polyhedra found in this crystal structure are listed in Tables 3 and 4. These parameters were analyzed using VaList (8) to determine the proper oxidation states of the constituent cations. The results from this analysis are listed in Table 5. All of the bond valence calculations agree to within roughly 10% of the formal oxidation states of $+3$, $+5$, and $+2$ on the lanthanum, rhenium, and manganese sites, respectively.

An interesting comparison can be made with the nearly isostructural $La_5Mo_4O_{16}$. The stacking is nearly identical in this material, with two distinct alternating layers of corner-sharing Mo octahedra and edge-sharing Mo–Mo bioctahedra. The difference in these two materials is that the replacement of Mo by Mn and Re in the corner-shared octahedral layer results in a distortion away from monoclinic to pseudomonoclinic (*C*-1 triclinic) symmetry. The positioning of the Re and Mn atoms in this layer is interesting, since Ledesert found through bond valence analysis that the two Mo sites displayed slightly lower and higher oxidation states than the commonly accepted $+4$ value (with reported values of 3.84 and 4.68) (5). The Mn and Re atoms in our structure occupy the sites of lower and higher oxidation states, respectively, in $La_5Re_3MnO_{16}$, reinforcing the close structural relationship of these compounds.

TABLE 3

La(1)–O(2)	2.415(4)	La(3)–O(1)	2.614(4) × 2
O(3)	2.463(5)	O(2)	2.411(4) × 2
O(4)	2.527(5)	O(5)	2.553(4) × 2
O(5)	2.536(5)	O(6)	2.564(4) × 2
O(6)	2.635(4)		
O(7)	2.570(5)	Re(1)–O(1)	1.968(4)
O(7)	2.536(5)	O(1)	2.051(4)
O(8)	3.002(5)	O(2)	1.947(4)
		O(3)	2.057(4)
La(2)–O(2)	2.461(4)	O(5)	1.907(4)
O(3)	2.425(4)	O(6)	1.916(4)
O(4)	2.463(4)		
O(5)	2.572(4)	Re(2)–O(4)	1.907(5) × 2
O(6)	2.584(5)	O(7)	1.996(4) × 2
O(8)	2.420(5)	O(8)	1.971(5) × 2
O(8)	2.847(5)		
		Mn–O(3)	2.131(5) × 2
Re(1)–Re(1)	2.4068(5)	O(7)	2.123(4) × 2
		O(8)	2.182(4) × 2

TABLE 4

O(1)–Re(1)–O(1)	106.5(1)	Re(1)–O(3)–Mn	148.2(2)
O(2)–Re(1)–O(5)	90.6(2)		
O(1)–Re(1)–O(5)	87.8(2)	Re(2)–O(7)–Mn	154.3(3)
O(2)–Re(1)–O(3)	86.3(2)		
O(6)–Re(1)–O(3)	81.0(2)		
O(4)–Re(2)–O(8)	88.4(2)	O(3)–Mn–O(7)	85.6(2)
	91.6(2)		94.4(2)
O(4)–Re(2)–O(7)	88.4(2)	O(3)–Mn–O(8)	85.3(2)
	91.6(2)		94.7(2)
O(7)–Re(2)–O(8)	89.9(2)	O(7)–Mn–O(8)	89.6(2)
	90.1(2)		90.4(2)

One can also compare this structure with other pervoskite-related transition metal oxides. The reduced neodymium titanate, $Nd_3Ti_4O_2$ (6), for example, crystallizes in a similar structure with a pervoskite-like TiO_6 corner-sharing octahedral bilayer and a Ti_2O_{10} edge-shared octahedral layer. The Nd atoms lie in chains in the framework much like the La atoms in $La_5Re_3MnO_{16}$. An important difference in the two structural types is the manner in which the Ti octahedra are connected. Instead of having their apexes connected to the Ti_2O_{10} layer, the TiO_6 octahedra are linked by their four equatorial ligands to the next layer and have their apexes linked to other TiO_6 octahedra that lie in chains in the network. The two structures both have extremely short metal–metal bonds, though, with Ti–Ti distances of 2.760(3) Å. Resistivity measurements on this material have shown that it is indeed nonmetallic, and thus there is localization of free electrons in the structure that is more than likely due to the Ti–Ti bond. A similar measurement in our material would be crucial to determining the nature of the bonding in the Re–Re bioctahedra and characterizing the magnetic response.

TABLE 5

Cation	Valence	Cation–oxygen bond valence							
		O(1)	O(2)	O(3)	O(4)	O(5)	O(6)	O(7)	O(8)
La(1)	2.8	—	0.52	0.46	0.38	0.37	0.29	0.37	0.11
		—	—	—	—	—	—	0.34	—
La(2)	2.8	—	0.46	0.50	0.46	0.34	0.33	—	0.51
		—	—	—	—	—	—	—	0.16
La(3)	3.1	0.30	0.52	—	—	0.36	0.35	—	—
		0.30	0.52	—	—	0.36	0.35	—	—
Re(1)	4.5	0.75	0.79	0.59	—	0.88	0.86	—	—
		0.60	—	—	—	—	—	—	—
Re(2)	4.6	—	—	—	0.88	—	—	0.69	0.74
		—	—	—	0.88	—	—	0.69	0.74
Mn	2.3	—	—	0.40	—	—	—	0.41	0.35
		—	—	0.40	—	—	—	0.41	0.35
O	Valence	−2.0	−2.3	−2.0	−1.7	−2.0	−1.8	−1.8	−1.9

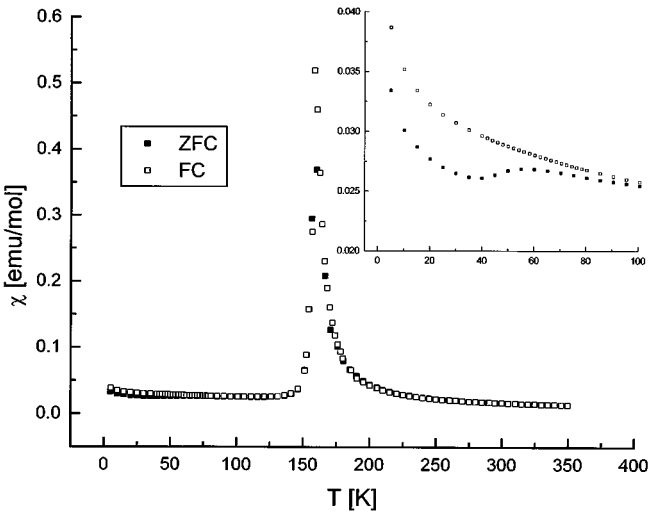

FIG. 5. The magnetic susceptibility as a function of temperature for an applied field of 0.05 T. Note the divergence in the FC and ZFC runs at low temperatures in the insert.

Magnetism in $La_5Re_3MnO_{16}$

Perovskite and pervoskite-related materials often exhibit fascinating low-temperature magnetic behavior that is commonly due to the layered stacking of the magnetic species. To investigate these properties, the magnetic susceptibility of single phase powder samples of $La_5Re_3MnO_{16}$ was measured. The magnetic susceptibility of polycrystalline $La_5Re_3MnO_{16}$ is displayed in Figs. 5 and 6 for a field of 0.05 T. There are clearly three features of interest in the

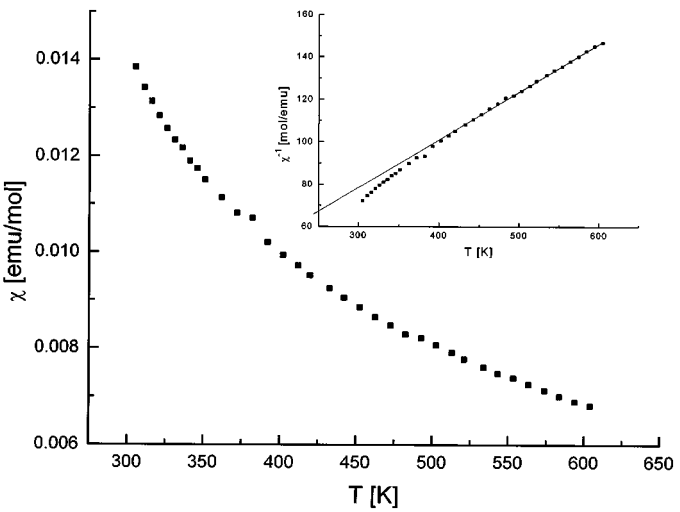

FIG. 6. The high-temperature magnetic susceptibility as a function of temperature for an applied field of 0.05 T. The insert shows the inverse susceptibility with a linear regression based upon the Curie–Weiss law (2), which gives a Curie constant of 4.43(4) emu·K/mol (corresponding to $S = 2.52(2)$) and a Weiss temperature of $\theta = -48(5)$ K.

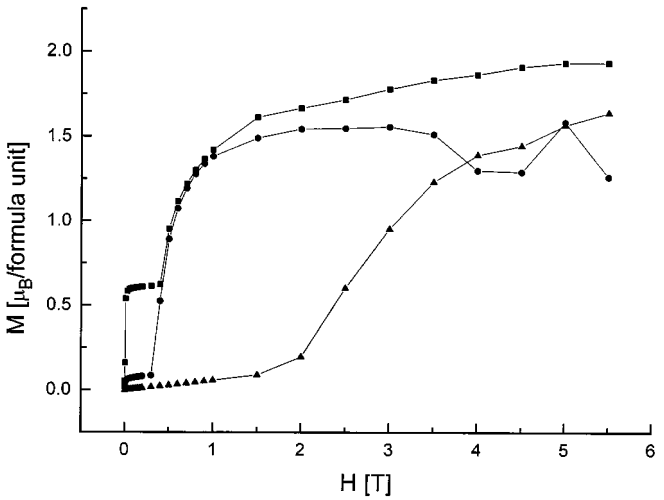

FIG. 7. Magnetization as a function of applied field for 5 K (▲), 60 K (■), and 120 K (●).

response: (1) a low-temperature phase of possible short-range magnetic ordering at temperatures lower than about 50 K, as evidenced by the difference in the FC and ZFC data, (2) a magnetic transition at about 160 K, and (3) Curie–Weiss behavior in the range 400–600 K. Figure 6 shows this high-temperature response more explicitly. The high-temperature data can be fit to the Curie–Weiss law

$$\chi = C/(T - \theta_c) \qquad [2]$$

where χ is the molar susceptibility, C is the Curie constant, and θ_c is the Weiss temperature. The Curie constant was found to be 4.43(4) emu · K/mol, which is consistent with Mn^{2+} ($S = 5/2$) as the only magnetic species (the spin-only Curie constant is 4.375 emu · K/mol for $S = 5/2$). The Weiss temperature of $\theta_c = -48(5)$ K indicates the presence of antiferromagnetic coupling between the moments.

In an effort to understand further the magnetic susceptibility measurements, the magnetization of the sample as a function of magnetic field was measured for three temperatures: 5, 60, and 120 K (see Fig. 7). At 5 K, the response indicates antiferromagnetic alignment of the moments up until a field of about 2 T, beyond which the magnetization grows more rapidly to a value of 1.6 μ_B at about 5.5 T. At 60 and 120 K, however, there is a notable difference in the magnetic response. At both temperatures, there is an initial sharp rise in the magnetization, followed by a plateau to about 0.4 T. After this critical field has been reached, there is another sharp rise to apparent saturation at about 2 μ_B by 2 T. The maximum saturation moment for Mn^{2+} ($S = 5/2$) is 5 μ_B. These observations point to a complex magnetic structure and H–T phase diagram for this material.

Other aspects of the magnetism are also puzzling at this stage. For example there is apparently no contribution from Re^{5+} to the magnetic suceptibility. In a localized electron picture, Re^{5+} is an $S = 1$ ion and a spin-only Curie constant of 1.00 emu · K/mol Re^{5+} would be expected, although this value may be reduced by spin–orbit coupling.

One can imagine at least two mechanisms by which the Re^{5+} moments might be quenched, multiple bond formation and electron delocalization. For example, the Re(1) atoms reside in the bilayer consisting of edge-sharing Re–O octahedra with very short Re–Re distances, as noted previously. It is natural to propose the existence of Re–Re double bonds that would provide moment quenching for these sites. This seems to be a likely scenario, as the bond distance of 2.4068 Å is consistent with double bonds of length 2.42 Å (9). Other systems exist that have this Re–Re bonding in edge-shared bioctahedra (10). Of particular relevance is the system $K_4[Re_2O_2(C_2O_4)_4] \cdot 3H_2O$, which has Re–Re edge-shared octahedra with oxygen ligands. The metal–metal distance has been reported at 2.36 Å (11), which is comparable to the Re–Re distance in $La_5Re_3MnO_{16}$. The shorter bond distance and lower oxidation state (+4) in this case indicates the presence of a triple bond. Since the Re–Re bond distance in $La_5Re_3MnO_{16}$ is slightly longer, it is more probable that there is double bonding on the Re(1) site involving a $5d^2$–$5d^2$ interaction.

The next issue concerns the electrons on the Re(2) site. One can imagine that if a pathway can be devised to delocalize the electrons on this site, then the Re d electrons that are not involved with the Re–Re double bonds form a Fermi surface (of, no doubt, quite a complex topology) and, thus, the compound should be metallic. While there is no direct evidence for this hypothesis, the magnetic properties, especially the relatively high transition temperature, provide indirect support. For example given the dilute nature of the Mn^{2+} magnetic centers, that the Mn-containing layers are well separated by 10.24 Å and the fact that no Mn–O–Mn superexchange pathways exist, it is very difficult to understand a critical temperature as high as 160 K without the intervention of a conduction electron mediated spin coupling mechanism such as RKKY.

As a counter argument to the above, one should note that there are no Re(2)–O–Re(2) connections in the pervoskite layer or with the Re_2O_{10} units; only Re(2)–O–Mn–O–Re(2) or Re(2)–O–Mn–O–Re(1) pathways exist. In similar materials, there is evidence for local moments on the Re ions (12). Thus, if there is a local moment on Re(2), one must consider a ferrimagnetic model for the Re(2)–Mn layers. The magnetization results lend some support to this, as the saturation of the moment only reached about 2 μ_B per formula unit, which is shy of the value expected for Mn^{2+} (5 μ_B). The ordering at 160 K would then involve a crossover from 2d to 3d magnetic order. The low-temperature FC–ZFC irreversibility might result from a spin canting. There are very few examples of layered ferrimagnetic materials and these hypotheses merit further investigation.

Elements of the above models can be verified by further studies. For example neutron diffraction can determine if all of the ordered magnetic moment is associated with the Mn sites and transport or optical measurements would disclose metallic behavior.

ACKNOWLEDGMENTS

The authors express their gratitude to Professor I. D. Brown, who assisted with the bond valence calculations, and to M. Bieringer, who assisted with the powder synthesis. C. R. Wiebe gratefully acknowledges support for this work from the Natural Sciences and Engineering Research Council in the form of a PGS B. This project was also supported through a research grant to J. E. Greedan through the Natural Sciences and Engineering Research Council.

REFERENCES

1. R. J. D. Tilley, *Endeavor* **14,** 124 (1990).
2. R. M. Hazen, *Sci. Am.* **358,** 52 (1988).
3. J. G. Bednorz and K. A. Müller, *Z. Phys. B* **64,** 189 (1986).
4. N. L. Morrow and L. Katz, *Acta Crystallogr. B* **24,** 1466 (1968).
5. M. Ledesert, Ph. Labbe, W. H. McCarroll, H. Leligny, and B. Raveau, *J. Solid State Chem.* **105,** 143 (1993).
6. B. Hassen, S. A. Sunshine, T. Siegrist, and R. B. Van Dover, *J. Solid State Chem.* **105,** 107 (1993).
7. A. Perrin and M. Sergent, *New J. Chem.* **12,** 337 (1988).
8. A. S. Willis, VaList for GSAS, 1998.
9. F. A. Cotton, *Inorg. Chem.* **4,** 334 (1965).
10. F. A. Cotton and R. A. Walton, "Multiple Bonds between Metal Atoms." Wiley and Sons, New York, 1982.
11. T. Lis, *Acta Crystallogr. B* **31,** 1594 (1975).
12. A. W. Sleight, J. Longo, and R. Ward, *Inorg. Chem.* **1,** 245 (1962).